Investigation of the origin of deep levels in CdTe doped with Bi

E. Saucedo,[1,a)] J. Franc,[2] H. Elhadidy,[2] P. Horodysky,[2] C. M. Ruiz,[3] V. Bermúdez,[3] and N. V. Sochinskii[4]
[1]*Material Physic Department, Universidad Autónoma de Madrid, Ctra. Colmenar km 14, 28049 Madrid, Spain*
[2]*Faculty of Mathematics and Physics, Institute of Physics, Charles University, Ke Karlovu 5, CZ 121 16 Prague, Czech Republic*
[3]*IRDEP, Institute of Research and Development of Photovoltaic Energy (UMR 7174, CNRS/EDF/ENSCP), 6 Quai Watier, BP 49, 78401 Chatou cedex, France*
[4]*Instituto de Microelectrónica de Madrid-CNM-CSIC, c/Isaac Newton 8 (PTM), Tres Cantos, 28760 Madrid, Spain*

(Received 6 September 2007; accepted 5 February 2008; published online 1 May 2008)

Combining optical (low temperature photoluminescence), electrical (thermoelectric effect spectroscopy), and structural (synchrotron X-ray powder diffraction) methods, the defect structure of CdTe doped with Bi was studied in crystals with dopant concentration in the range of $10^{17}-10^{19}$ at./cm^3. The semi-insulating state observed in crystals with low Bi concentration is assigned to the formation of a shallow donor level and a deep donor recombination center. Studying the evolution of lattice parameter with temperature, we postulate that the deep center is formed by a Te–Te dimer and their formation is explained by a tetrahedral to octahedral distortion, due to the introduction of Bi in the CdTe lattice. We also shows that this model agrees with the electrical, optical, and transport charge properties of the samples. © *2008 American Institute of Physics*. [DOI: 10.1063/1.2903512]

I. INTRODUCTION

The most important pre-requisites for applying CdTe crystals as x- and gamma ray detectors is that the material has a high electrical resistivity with adequate transport charge properties.[1,2] Deep levels play a key role on the electrical and transport charge properties of CdTe, determining the final detector's performance.[3–6]

For example, has been demonstrated that the presence of these recombination deep centers is the mainly reason of the polarization effect of detectors, leading to the collapse of their internal electric field. The mechanism has been interpreted by the accumulation of charges in these recombination centers.[7]

In fact, several deep centers have been reported in CdTe and assigned to different defects such as $Ge_{Cd}^{+/0}$ in CdTe:Ge,[8–10] $Sn_{Cd}^{+/0}$ in CdTe:Sn,[9,10] $Te_{Cd}^{+/0}$ in undoped CdTe, CdTe:Cl or CdTe:In,[5,6,10] for example. Their influence on the detector abilities was studied in Refs. 11 and 12. Nevertheless, there is a controversy about the actual origin of the different deep centers in CdTe, although it is generally accepted that mostly of them are recombination centers with complex structures.[5]

The energy levels in CdTe have been studied by optical and electrical techniques,[5,6,8–10] and their origin assigned to different impurities or defects present in the material. In contrast, there are no studies involving structural considerations and their influence on the defect structure.

Recently, the optical, electrical and photoconductive properties of CdTe crystals doped with the large-size-mismatched atom Bismuth, have been reported.[13,14] A Bi related center at $E_C-0.71$ eV was confirmed as the responsible for the semi-insulating state and high photosensitivity of the crystals. Nevertheless, the actual origin of the deep center is still unknown, but was suggested the posibility that large atomic displacements in large-size-mismatched doped materials (as is the case of Bi in CdTe), could be important in their formation.[15]

Thus, using a combination of low temperature photoluminescence (PL) in the 0.45–1.6 eV energy region, thermoelectric effect spectroscopy (TEES), and synchrotron x-ray powder diffraction (SXPD), we investigate the properties and origin of the deep levels in CdTe:Bi.

II. EXPERIMENTAL

CdTe:Bi doped crystals were grown by the vertical Bridgman method using different dopant concentrations from $10^{17}-10^{19}$ at./cm^3. Samples of $10\times10\times1.5$ mm^3 were cut, and then mechanically and chemically polished as was previously reported.[14] For TEES measurements, gold contacts were electrochemically deposited using a $AuCl_3$ solution (0.5*M*).

PL was performed using a Fourier transform infrared (FTIR) spectrometer Bruker IFS66/S with Si and InSb detectors in a spectral range (0.45–1.6 eV) at temperature of 4.8 K in a continuous flow He cryostat. He–Ne laser with power of 15 mW was used for excitation. Spectra were corrected with respect to sensitivity of the detectors.

TEES spectra were collected in the 90–400 K temperature range, using a home made cryostat controlled by a 3508 Eurotherm temperature controller, and measuring the thermoelectric current using a Keithley electrometer system

[a)]Author to whom correspondence should be addressed. Electronic mail: edgardo.saucedo@uam.es. Tel.: 0034914974784. Fax: 0034914978579

TABLE I. Bi concentration and resistivity at room temperature of the studied samples (N.D.=not detected).

Sample	Bi conc. (cm^{-3})	ρ (Ω cm)
Bi1	2×10^{17}	7×10^{9}
Bi2	6×10^{17}	5×10^{8}
Bi3	1.5×10^{18}	10^{7}
Bi4	8×10^{18}	10^{5}
Und.	N.D.	4×10^{4}

(Model 6514). The temperature gradient through the sample was measured using a differential thermocouple, connected to a Keithley 2000 source meter.

X-ray powder diffraction studies were performed in the Beamline 25 of the European Synchrotron Radiation Facility of Grenoble, France, under the experiments HS-3183 and HS-3184. For the analyses, samples were fully powdered (grain size less than 10 μm) and then introduced in a capillary of 300 μm in diameter. X-ray diffraction spectra were collected between 10° to 40° in theta, in a temperature range from 80 to 300 K. In this angle region, the (111), (220), (311), (400), (331), and (422) CdTe reflections were collected, and treated using the standard software, fitting the peaks to pseudo-Voigt functions. The synchrotron x-ray beam was collimated using a Si crystal, selecting a line with wavelength of 0.827 002 68 nm.

III. RESULTS

The electrical properties and Bi concentration of the studied samples are presented in Table I. As was reported previously,[14] resistivity changes five orders of magnitude when the Bi concentration increases from 10^{17} to 10^{19} at./cm^3. The reason of this change is explained by means of modifications in the defect levels structure. It was showed in Ref. 14 that Bi in low concentrations substitutes Cd (see also Ref. 15), leading to a semi-insulating state. When the Bi concentration exceeds a certain limit, the dopant preferentialy goes to Te sites and the resistivity falls down. The amphotheric behavior of Bi is able to explain the dependence of the resistivity with the Bi concentration.

First, we will concentrate our discussion on the photoluminescence results. Figure 1(a) shows the PL spectra in the energy region from 1.1 to 1.6 eV for samples Bi1, Bi4, and undoped (Und), while Fig. 1(b) shows a detail between 1.50 to 1.6 eV. Several changes are observed mostly in sample B1 with respect to the others. The (X) emission is clearly detected indicating a good sample quality. Also, a strong (D^0-X) emission and several (A^0-X) are observed, with their respective phonon replicas, as is denoted in Fig. 1(b). Concentrating our attention on the emission (D^0-X) and following the same procedure that Francou *et al.*,[16] the binding energy of the exciton (E_{loc}) and the ionization energy (E_i) were obtained (values are presented for the three studied samples and for typical donor impurities reported in the literature).

TABLE II. Characteristic parameters of the emission (D^0-X) for the three studied samples and for typical donor impurities extracted from the literature (E—energy position, E_{loc}—binding energy of the exciton, and E_i—ionization energy).

Donor	Parameter			
	E (eV)	E_{loc} (meV)	E_i (meV)	Ref.
D^0-X Und.	1.592 8	3.71	15.08	This work
D^0-X Bi1	1.592 6	4.37	17.76	This work
D^0-X Bi4	1.592 9	3.57	14.51	This work
F_{Te}	1.593 14	3.36	13.71	15
Ga_{Cd}	1.593 09	3.41	13.83	15
Al_{Cd}	1.593 05	3.46	14.04	15
In_{Te}	1.593 02	3.48	14.08	15
Cl_{Te}	1.592 96	3.54	14.48	15

From Table II, it is evident that the origin of the emission (D^0-X) for sample Bi1 does not correspond to the typical donor impurities studied in CdTe. Considering that this emission is directly related to the incorporation of Bi at low concentrations, their origin could be assigned to a defect related to the dopant, probably Bi replacing Cd. On the other hand, for samples Und and Bi4 the parameters of the (D^0-X) emission agree with the values of impurities such as In or Cl,[15] commonly present as contaminants in CdTe:Bi.[14] In fact, using mass spectroscopy, we detect In and, using x-ray fluorescence, Cl in both samples.

The (A^0-X) emissions dominate the spectra for Und and Bi4 samples as is clearly observed in Fig. 1(b). Three emissions are detected, which can be assigned to typical acceptor defects or impurities present in CdTe, such as V_{Cd}, Na, and Ag.[17–22] Thus, changes from pure (D^0-X)-type spectrum for Bi1 sample, to a (A^0-X)-type spectrum for samples Bi4 and Und indicate that the donor involved in the first case is important in the electrical compensation. This shallow defect is

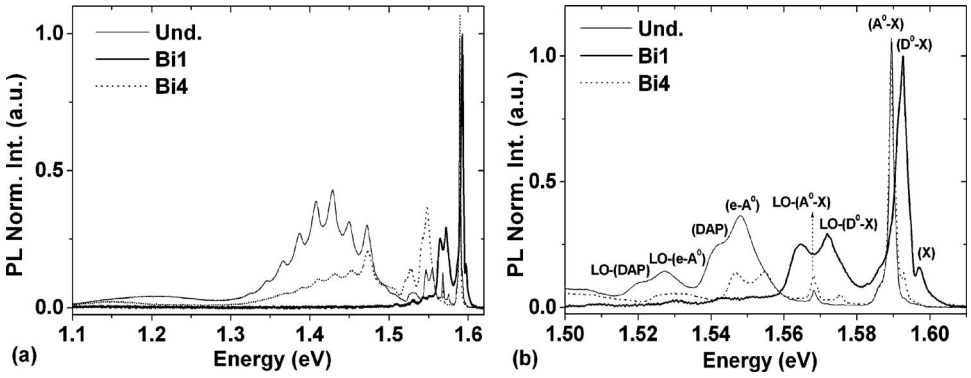

FIG. 1. PL spectra at 4 K for the different studied samples in the energy region between 1.1 and 1.6 eV (a) and a detail between 1.5 and 1.6 eV (b).

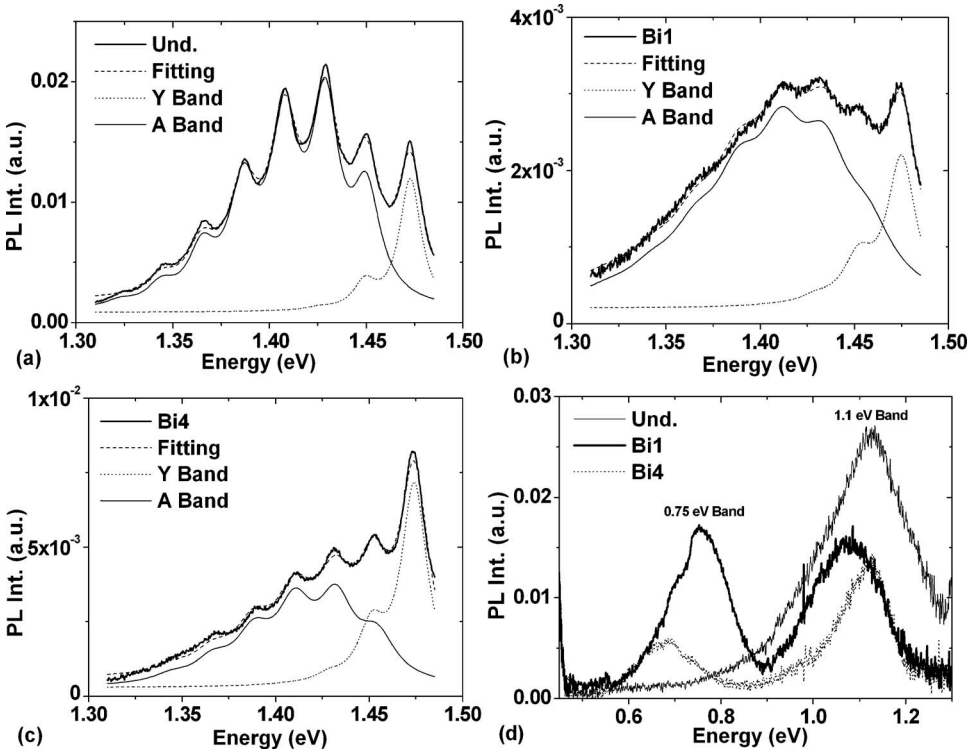

FIG. 2. PL spectra at 4 K for the different studied samples in the energy region between 1.3 and 1.5 eV for the samples Und (a), Bi1 (b), and Bi4 (c), with the fitting to two bands (*A* and *Y* bands), and the spectra of the three samples in the energy region between 0.45 and 1.3 eV (d).

not able to explain completely the electrical properties of semi-insulating CdTe:Bi crystals,[13,14] being necessary to study the deep levels.[14]

The other important emission in the spectra is a complex band centered at 1.55 eV, which is absent in sample Bi1 and shifted to higher energies in sample Bi4 with respect to the undoped [see Fig. 1(b)]. The origin of this band is the combination of two emissions: a donor-acceptor pair (DAP) transition at low energies and recombination of free electrons in uncharged acceptor impurity $(e-A^0)$ at high energies. Studying the band as in Ref. 23, the ionization energy (E_{i-A}) of the acceptor involved in the $(e-A^0)$ emission was calculated. For the Und sample, a value of E_{i-A} of 51.4 meV was obtained (at 1.5549 eV), which is in correspondence with values accepted for complexes formed by impurities commonly present in the material, such as $(V_{Cd}-Al_{Cd})^0$ or $(V_{Cd}-Cl_{Te})^0$.[24,25] In the case of Bi4 sample, the value of a E_{i-A} is 58.2 meV [the $(e-A^0)$ peak is at 1.5482 eV]. It does not correspond, neither to a typical impurity,[24,25] nor to other V group impurities (N, P, As, and Sb).[23,26] Thus, it is possible to infer that the uncharged acceptor involved in the 1.55 eV band in the sample Bi4 is related to Bi, presumably due to the defect: Bi_{Te}^0.

The other part of the photoluminescence spectra is shown in Fig. 2, where the 1.4 eV band is observed for Und, Bi1, and Bi4 samples in the Figs. 2(a)–2(c), respectively. The fitting of this broad emission was done using the Huang–Rhys equation[27] and defining two bands: the *A* band formed by a complex between V_{Cd} and shallow donors and the *Y* band which arises from the exciton recombination in defects such as dislocations.[28,29] Very good agreement between the experimental and theoretical values is obtained and the parameters extracted from the fitting procedure,[27] including the Huang–Rhys parameter (*S*), the energy of the zero phonon line (E_{Z0}), the phonon energy (E_{Ph}), and the ionization energy of the donor involved in the *A* band, are presented in Table III.

The *Y* band is pressumably related to defects associated to the dislocations which have a low *S* parameter. Studying the *A* band in samples Und and Bi4, we obtain similar results indicating that can have the same origin. In fact, the values of *S* and E_{Z0} could be assigned to donor impurities such as Ga or In.[27] The most interesting results are obtained for sample Bi1, which have a smoother and weaker *A* band with a high *S* value. The donor involved in the *A* band does not correspond to the different donor impurities reported in the literature.[27] Then, we can infer that Bi plays a role in the *A* band, presumably means a complex involving the same donor defect previously described: Bi_{Cd}.

The last part of the spectra is presented in Fig. 2(d). Two broad bands are clearly observed at ~1.1 and 0.75 eV. The 1.1 eV band which is present in the three samples has been extensively studied[30,31] and we will not discuss about it here.

TABLE III. Characteristic parameters of the *A* and *Y* bands extracted from the fitting to the Huang–Rhys equation.

		Sample		
Band	Parameter	Und	Bi1	Bi4
Y	E_{Z0} (eV)	1.4728	1.4750	1.4741
	E_F (meV)	23.51	22.89	22.84
	S	0.19	0.28	0.26
A	E_{Z0} (eV)	1.4501	1.4572	1.4543
	E_F (meV)	21.26	22.97	22.04
	S	1.84	2.15	1.84
	E_B (meV)	138.9	116.7	128.3

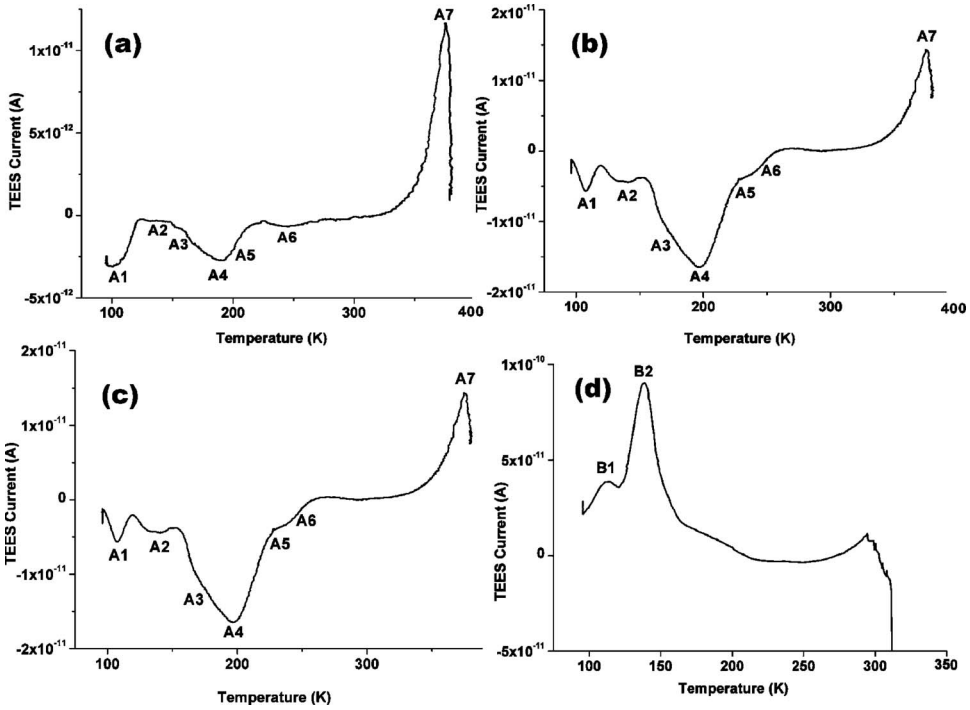

FIG. 3. TEES spectra of several CdTe:Bi samples: (a) Bi1, (b) Bi2, (c) Bi3, and (d) Bi4 (Temperature rate of 0.083 K/s).

On the other hand, the PL band close to the middle of the CdTe band gap is absent in the Und sample, being very intense in Bi1 and diminishing their intensity for Bi4. This is an indication that the deep center responsible for this emission is related to Bi. Clearly, the energy position and shape of the band are not the same for both samples, implying a different origin or changes of their structure. In the case of Bi1, this center is responsible for the semi-insulating state,[14] having a donor character. Taking into account that Bi introduces a shallow donor level, it is hard to believe that this deep center is formed by a simple structure. More probably, it is a recombination center with a complex structure.

To study the deep center, TEES measurements were performed on samples Bi1 to Bi4, as can be observed in Fig. 3. Several methods are available in Ref. 32 for deriving the trap's ionization energy and we have preferred applying the initial rise method[33] to our TEES curves. This method is independent of the recombination mechanism and in practice only the initial portion of the peak is evaluated. The extracted thermal energy values (E_t) with the corresponding maximum temperature (T_M) are used to calculate the trapping capture cross section according to the following equation (the heating rate method):[33]

$$\sigma = (\beta E_t / C m^* T_M^4)\exp(E_t/kT_M), \quad C = 4k^3\sqrt{6\pi^3}/h^3,$$

where β is the heating rate and m^* is the effective mass of the charge carrier. In CdTe $m^*=0.096m_0$ for electron and $m^*=0.83m_0$ for holes, with m_0 being the electron rest mass and h is Planck's constant.

The energy, capture cross sections, and character of the centers are presented in Table IV. Semi-insulating samples (Bi1 and Bi2) have similar spectra with a group of electron trap centers (A1 to A5 in Figures 3(a) and 3(b).) and a hole trap center (A7). The intensity of peaks A3 and A4 increase when the center A7 vanish, for low resistivity samples. This is an indication that the A7 center is important in the electrical compensation process, and the group of electron traps, mostly the A3 and A4, are partially responsible for the resistivity decrease. See, for example, in sample Bi3 that the peak A7 is very low and the peaks A3 and A4 dominate the spectrum, and in consequence, the resistivity diminish with respect to samples B1 and B2.

The energy (0.73 eV) and the capture cross section ($\sigma = 5\times10^{-14}$ cm^{-2}) of the A7 center obtained by TEES, is in agreement with the values reported by Photo Induced Current Transient Spectroscopy (PICTS) measurements on the same samples,[14] but the origin of this deep center is still unknown. Then, to propose a possible structure of the A7 center, we must to take into account their donor character with unusual holes trap properties.

The defect structure of sample Bi4 is completely different to the others [see Fig. 3(d)]. In this case, the most important defect is a hole trap with an activation energy of 0.31 eV and a capture cross section of 8×10^{-17} cm^2 as is presented in Table IV. This deep acceptor center is the responsible of the low resistivity of sample Bi4, and can be unambiguously assigned to the defect $Bi_{Te}^{-/0}$.[14]

TABLE IV. Summary of the peaks detected in TEES spectra of Fig. 3.

Peak	Energy (eV)	σ (cm^2)	Character
A1	0.14	2×10^{-18}	Electron trap
A2	0.32	7×10^{-17}	Electron trap
A3	0.29	1.6×10^{-18}	Electron trap
A4	0.37	4.5×10^{-17}	Electron trap
A5	0.61	1.4×10^{-11}	Electron trap
A6	0.43	3×10^{-17}	Electron trap
A7	0.73	5×10^{-14}	Hole trap
B1	0.07	3×10^{-16}	Hole trap
B2	0.31	8×10^{-17}	Hole trap

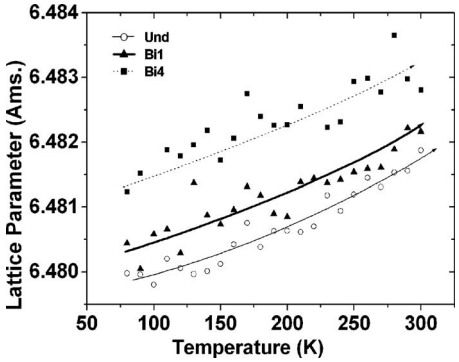

FIG. 4. Evolution of the CdTe lattice parameter with the temperature for the three studied samples (Und, Bi1, and Bi4).

Concerning the properties of the A7 center in CdTe:Bi doped samples (Bi1), it has been reported that the optical absorption spectrum has two peculiarities.[14] The first is a broad absorption band from 1700 nm to the absorption edge, corresponding to a transition between a localized state and an extended state (the valence or conduction bands). The second important observation is the redshift of the absorption edge for Bi1 sample, with respect to the undoped. In the spectra of sample Bi4, the absorption edge shifts newly to lower wavelengths and the spectrum is very similar to the undoped crystal.[14] This wavelength shift of the absorption edge for low dopant concentration is unusual in semiconductors. Nevertheless, the same redshifts was observed in MgO crystals doped with Au,[34–36] and assigned to the charge transfer between Au aggregates formed by two or three atoms and a V_{Mg}.[34–36]

In our samples, a possible explanation of the redshift to the fundamental absorption edge is the formation of Te aggregates induced by the presence of Bi. It is important to notice that, as has been demonstrated in other II-VI semiconductors such as ZnSe or ZnS, that the formation of bulk instability, in particular, VI-VI dimmers (Se–Se), is effective in acceptor passivation.[37–39] This means that if we are able to show the formation of Te dimmers in large-seze-mismatched CdTe, using a modification of the model of Park and Chadi,[37] we could explain the red shift of the absorption edge[14] and the structure of the deep donor level which is very important in the acceptor passivation.[14]

For this purpose, we have done synchrotron x-ray powder diffraction on samples Und, Bi1, and Bi4 under the experiments HS-3183 and HS-3184, with the aim to study the variation of the CdTe lattice parameter and the Te sublattice, as functions of Bi concentration. The evolution of the CdTe lattice parameter (a) with the temperature for the three samples is shown in Fig. 4. The relationship $a_{Und} \leqslant a_{Bi1} \leqslant a_{Bi4}$ is observed in the whole temperature range (80 K $\leqslant T \leqslant$ 300 K), implying the expansion of CdTe lattice with the incorporation of Bi. This result is not surprising because of the large Bi radius. From Fig. 4, it is possible to estimate the thermal expansion coefficient (α) and compare it with the values reported in the literature. These parameters are summarized in Table V, where α for the Und sample is in agreement with the values accepted for undoped CdTe in this temperature range.[17,39] Conversely, α drastically diminishes for samples Bi1 and Bi4, at values as low as 1.70 K^{-1}, indicating that the presence of Bi induces this reduction.

TABLE V. Thermal expansion coefficient for the three studied samples and values extracted from the literature.

Material	$\alpha \times 10^6$ (1/K)	T (K)	Reference
Und	3.75 ± 0.15	240	This work
Bi1	2.82 ± 0.20	240	This work
Bi4	1.70 ± 0.24	240	This work
CdTe undoped	3.9	200	17
CdTe undoped	4.6	293	17
CdTe undoped	4.3	240	39

Results can be interpreted by means of two effects: first, the reduction in the symmetry of the system due to the big size of Bi atoms, which strongly distort the CdTe lattice (isotropy loss); The second effect is the approach of two Te atoms and the formation of Te–Te dimers, reinforcing the bonding energy in the Te sublattice and reducing the thermal expansion coefficient, supported by the optical absorption measurements.[14] In such case, the variation of the interplanar distance with temperature could provide interesting information. In Table VI the interplanar distortion for the six studied planes are presented.

It is evident from Table VI that the interplanar distortion is strongly reduced mostly in planes with high Te density, being an indication of binding reinforcement between the neighbors Te atoms. The formation of this bulk instability can be described by a simple model, where the Bi_{Cd} donor defect induces a distortion in their first Te coordination sphere. In CdTe, Cd is surrounded by four Te atoms in a tetrahedral coordination sphere; whereas in Bi_2Te_3, Bi is surrounded by six Te atoms in an octahedral coordination sphere.[40] When Bi replaces Cd, the tetrahedral to octahedral distortion induces the approach of two Te atoms forming the Te dimmers, which explains the redshift of the absorption edge and the formation of the deep donor level.[37–39] The possible formation mechanism of the Te–Te dimers is presented in Fig. 5.

IV. CONCLUSION

The electrical and optical properties of CdTe doped with Bi were explained using structural considerations. Semi-insulating state in crystals with Bi concentration of approxi-

TABLE VI. Inter-planar distortion with the temperature for the following reflections in the CdTe x-ray powder diffraction pattern: (111), (220), (311), (400), (331), and (442).

Plane	Plane composition	Interplanar distortion (Å/K) $\times 10^6$		
		Und	Bi1	Bi4
(111)	50%Cd, 50%Te	6.29 ± 1.30	5.54 ± 1.60	5.4 ± 3.8
(220)	66.7%Cd, 33.3%Te	3.76 ± 0.32	3.85 ± 0.32	3.5 ± 0.20
(311)	100%Te	3.05 ± 0.15	2.07 ± 0.26	1.93 ± 0.29
(400)	100%Cd	2.58 ± 0.40	2.39 ± 0.21	2.30 ± 0.26
(331)	100%Te	2.74 ± 0.14	2.48 ± 0.13	1.78 ± 0.22
(442)	100%Te	2.17 ± 0.05	1.72 ± 0.08	1.77 ± 0.10

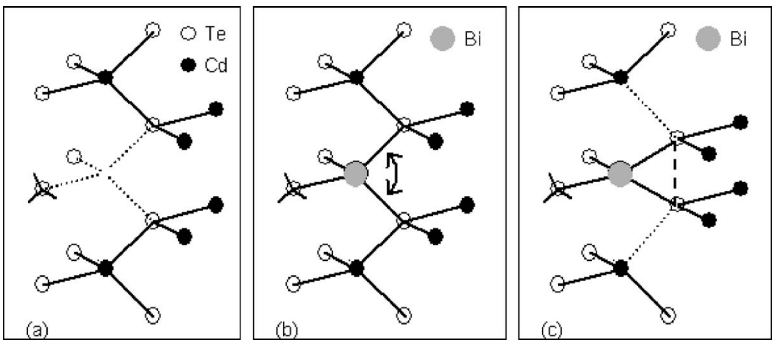

FIG. 5. Possible mechanism of the formation of a Te–Te dimmer by means of a tetrahedral to octahedral distortion. Introduction of Bi in a Cd vacancy (a); tetrahedral to octahedral distortion of the Te coordination sphere and the approach of the Te neighbors atoms (b) and formation of a Te–Te dimer (c) (the dashed line represents the bonding between two Te atoms).

mately 10^{17} at./cm^3 is assigned to both: the formation of a shallow donor level observed by PL measurements and, mainly, to a deep donor recombination center observed by PL and TEES measurements, which has donor character and hole trap properties. The donor part of the deep center is interpreted by the formation of Te–Te dimers as consequence of the tetrahedral to octahedral distortion of the first Te coordination sphere around Bi, using a modification of the theoretical model presented by Park and Chadi.[37] We demonstrate that in large-size-mismatched doped semiconductors, atomic displacements around the dopant are very important in the electrical and optical properties.

ACKNOWLEDGMENTS

This work has been partly supported by the projects CAM SENSORCDT S-0505/MAT/0209, CAM FOTOFLEX S-0505/ENE-123, and EU FP6 PHOLOGIC 017158. The authors are grateful to the European Synchrotron Radiation Facility (ESRF) for the experiments HS-3183 and HS-3184 and to Dr. German Castro. E.S. also thanks to the MEC of Spain for the fellowship FPU 2003-1388.

[1]C. Szeles, Phys. Status Solidi B **241**, 783 (2004).
[2]C. Scheiber, Nucl. Instrum. Methods Phys. Res. A **380**, 385 (1996).
[3]M. Fiederle, C. Eiche, M. Salk, R. Schwarz, K. W. Benz, W. Stadler, D. M. Hofmann, and B. K. Meyer, J. Appl. Phys. **84**, 6689 (1998).
[4]A. Castaldini, A. Cavallini, B. Fraboni, P. Fernandez, and J. Piqueras, J. Appl. Phys. **83**, 2121 (1998).
[5]A. Cavallini, B. Fraboni, and W. Dusi, IEEE Trans. Nucl. Sci. **52**, 1964 (2005).
[6]J. Franc, V. Babentsov, M. Fiederle, E. Belas, R. Grill, K. W. Benz, and P. Höschl, IEEE Trans. Nucl. Sci. **51**, 1176 (2004).
[7]J. Franc, R. Grill, J. Kubát, E. Belas, P. Moravec, and P. Höschl, IEEE Trans. Nucl. Sci. **54**, 864 (2007).
[8]M. Fiederle, V. Babentsov, J. Franc, A. Fauler, K. W. Benz, R. B. James, and E. Cross, J. Cryst. Growth **243**, 77 (2002).
[9]M. Fiederle, A. Fauler, J. Konrath, V. Babentsov, J. Franc, and R. B. James, IEEE Trans. Nucl. Sci. **51**, 1864 (2004).
[10]M. Fiederle, V. Babentsov, J. Franc, A. Fauler, and J. P. Konrath, Cryst. Res. Technol. **38**, 588 (2003).
[11]B. Fraboni, A. Cavallini, and W. Dusi, IEEE Trans. Nucl. Sci. **51**, 1209 (2004).
[12]B. Fraboni, A. Cavallini, N. Auricchio, W. Dusi, M. Zanarini, and P. Siffert, IEEE Trans. Nucl. Sci. **52**, 3085 (2005).
[13]E. Saucedo, L. Fornaro, N. V. Sochinskii, A. Cuña, V. Corregidor, D. Granados, and E. Diéguez, IEEE Trans. Nucl. Sci. **51**, 3105 (2004).
[14]E. Saucedo, C. M. Ruiz, V. Bermúdez, E. Diéguez, A. Zappettini, E. Gombia, A. Baraldi, and N. V. Sochinskii, J. Appl. Phys. **100**, 104901 (2006).
[15]S. Limpijumnong, S. B. Zhang, S. H. Wei, and C. H. Park, Phys. Rev. Lett. **92**, 155504 (2004).
[16]J. M. Francou, K. Saminadayar, and J. L. Pautraut, Phys. Rev. B **41**, 12035 (1990).
[17]S. H. Song, J. F. Wang, and M. Isshiki, J. Cryst. Growth **257**, 231 (2003).
[18]*Narrow gap cadmium-based compounds*, edited by P. Capper, Emis Data Reviews Series Vol. 10, 1st ed., (Inspec, London, England, 1994), Cap. B2.2 and B6.4.
[19]J. P. Chamonal, E. Molva, and J. L. Pautrat, Solid State Commun. **43**, 635 (1982).
[20]E. Molva, J. P. Chamonal, and J. L. Pautrat, Phys. Status Solidi B **109**, 635 (1982).
[21]E. Molva, J. L. Pautrat, K. Samindanayar, G. Milchberg, and N. Magnea, Phys. Rev. B **30**, 3344 (1984).
[22]E. Molva and L. S. Dang, Phys. Rev. B **27**, 6222 (1983).
[23]E. Molva, K. Saminadayar, J. L. Pautraut, and E. Ligeon, Solid State Commun. **48**, 955 (1983).
[24]S. H. Song, J. Wang, Y. Ishikawa, S. Setob, and M. Isshiki, J. Cryst. Growth **237–239**, 1726 (2002).
[25]R. O. Bell, Solid State Commun. **16**, 913 (1975).
[26]H. Kanie, K. Ogino, H. Kuwabara, and H. Tatsuoka, Phys. Status Solidi B **229**, 145 (2002).
[27]N. Armani, C. Ferrari, G. Salviati, F. Bissoli, M. Zha, A. Zappettini, and L. Zanotti, J. Phys.: Condens. Matter **14**, 13203 (2002).
[28]J. Schreiber, L. Höring, H. Uniewski, S. Hildebrandt, and H. S. Leipner, Phys. Status Solidi A **171**, 89 (1999).
[29]W. Stadler, D. M. Hofmann, H. C. Alt, T. Muschik, B. K. Meyer, E. Weigel, G. Müller–Vogt, M. Salk, E. Rupp, and K. W. Benz, Phys. Rev. B **51**, 10619 (1995).
[30]Z. Sobiesierski, I. M. Dharmadasa, and R. H. Williams, J. Cryst. Growth **101**, 599 (1990).
[31]Z. Sobiesierski, I. M. Dharmadasa, and R. H. Williams, Appl. Phys. Lett. **53**, 2623 (1988).
[32]J. Xu, J. Moxom, S. H. Oberbury, C. W. White, A. P. Mills, and R. Suzuki, Phys. Rev. Lett. **88**, 175502 (2002).
[33]K. H. Nicholas and J. Woods, Br. J. Appl. Phys. **15**, 783 (1964).
[34]P. K. Jain, S. Eustis, and M. A. El–Sayed, J. Phys. Chem. B **110**, 18243 (2006).
[35]*Photoelectronic properties of semiconductors*, edited by R. H. Bube (Cambridge University Press, Cambridge, 1992), pp. 149–188.
[36]N. Krsmanovic, K. G. Lynn, M. H. Weber, R. Tjossem, Th. Gessmann, Cs. Szeles, E. E. Eissler, J. P. Flint, and H. E. Glass, Phys. Rev. B, **62**, 279 (2000).
[37]C. H. Park and D. J. Chadi, Phys. Rev. Lett. **75**, 1135 (1995).
[38]D. J. Chadi and K. J. Chang, Appl. Phys. Lett. **55**, 579 (1989).
[39]D. J. Chadi and K. J. Chang, Phys. Rev. Lett. **61**, 873 (1988).
[40]*Semiconductors: Data Handbook*, edited by O. Madelung, 3rd edition (Springer, Berlin, 2004) Chap. 3.19, p. 232.